Removal of humic substances by the synergistic effect of biochar adsorption and activation of persulfate

Hongbo Liu, Mengting Ye, Xinyi Dong, Zhenxing Ren, Shiping Long, Eric Lichtfouse

Journal of Water Process Engineering 44 (2021) 102428

https://doi.org/10.1016/j.jwpe.2021.102428

Removal of humic substances by the synergistic effect of biochar adsorption and activation of persulfate

Hongbo Liu [a,*], Mengting Ye [a], Xinyi Dong [a], Zhenxing Ren [a], Shiping Long [b], Eric Lichtfouse [c]

[a] School of Environment and Architecture, University of Shanghai for Science and Technology, 516 Jungong Road, 200093 Shanghai, China
[b] Chongqing New World Environment Detection Technology Co. LTD, 22 Jinyudadao, 401122 Chongqing, China
[c] Aix-Marseille Univ, CNRS, IRD, INRA, Coll France, CEREGE, 13100 Aix en Provence, France

ARTICLE INFO

Keywords:
Adsorption
Oxidization
Corn stalk biochar
Humic acids (HA)
Persulfate (PS)

ABSTRACT

Combined adsorption and oxidation using biochar to activate persulfate has been recently applied to remove contaminants, yet most of the experiments are carried out using artificial synthetic water instead of real waters. Here we tested the removal of humic substances which is abundant and affecting water quality in natural waters, by persulfate combined with corn stalk biochar. Results showed that, compared with biochar prepared at 400 °C, 600 °C and 700 °C, biochar prepared at 900 °C after modified by hydrochloric acid had greater specific surface of 459.260 m^2/g, richer porosity and higher removal of humic acids of more than 80% at pH 5.0–9.0 in pure water. Treatment of real river water showed decrease of 80.4% and 69.7% of total organic carbon (TOC) and UV_{254}, respectively. The addition of tert-butyl-alcohol (TBA) and methanol (MeOH) inhibited the removal to a certain extent suggesting the existence of •OH and SO_4^{-}•. It was speculated that in addition to the adsorption of biochar, the oxygen-containing functional groups on its surface might act as active sites to promote the production of oxidized species. This work provides a method for corn stalks utilization in accordance with environmental sustainability and resource recovery.

1. Introduction

Humic substances such as soluble humic acids (HA), fulvic acids and insoluble humin, are major, complex, poorly known organic substances produced by the decay of living organisms in natural waters, wastewaters, soils and sediments [1–5]. Although humic substances themselves have few harmful effects on public health, they can induce sensory issues such as odor and bad taste in drinking water indirectly. Humic substances also favor the growth of phytoplankton in reservoirs [6]. An excess of dissolved organic matter in waters could also induce eutrophication and deaths of aquatic life. Furthermore chlorination of humic substances induces the formation of toxic by-products during water treatment [7], induced by the large number of functional groups in humic functions such as -C=O, -OH and -COOH [8]. Therefore, reducing the humic load before chlorination could decrease formation potential of disinfection by products.

Physical methods such as coagulation and membrane filtration were commonly used to remove humic substances, but with low efficiency, thus causing secondary pollution [9,10]. Chemical oxidation using advanced oxidation processes (AOPs) that generate reactive oxygen species (ROS) such as hydroxyl radicals, sulfate radicals, and alkoxyl radicals, especially the activation of persulfate (PS), peroxymonosulfate (PMS) and hydrogen peroxide (H_2O_2) are efficient in removing organic pollutants [11,12]. Persulfate is a focusing point of research and application due to its high stability, low cost, broader pH applicability, production of SO_4^{-}• with wider application, longer half-life time and similar oxidation potential as to •OH [13]. Persulfate can be activated by alkali, transition metal, ultraviolet, ultrasound and microwave. Improved humic removal could be achieved by oxidation and adsorption using biochar combined with persulfate.

Biochar are adsorbents produced by pyrolysis of organic materials such as agricultural residues, which are typically cheap, easy to obtain, metal-free, rich in oxygen-containing functional groups, porous of high specific surface area (SSA), and resistant to acid and alkali. Organic contaminants can be both adsorbed and oxidized using persulfate and biochar. There are many factors that affect the performance of biochar, including pyrolysis temperature, source of raw materials, modification methods and types of substrates to be removed. For example, 94.2%of norfloxacin was removed by persulfate and corn stalk biochar [14]. Egg shell biochar with persulfate achieved 90%of 2,4-dichlorophenol

* Corresponding author at: 516, Jungong Road, 200093 Shanghai, China.
E-mail address: Liuhb@usst.edu.cn (H. Liu).

removal via both free-radical and non-radical pathways [15]. The catalytic performance of biochar materials can be further improved by involving metals; for instance, Fe_3O_4 coated straw biochar increased the removal of tetracycline hydrochloride to more than 88% over a wide pH range of 3–11 [16]. Fe/Mn biochar achieved high-efficiency activation of persulfate for the removal of reactive blue 19 [17]. The specific reaction conditions and the introduction of biochar combined with persulfate to remove different organics in other literature were listed in the Table 1.

Most investigations on persulfate and biochar have been performed on pure compounds such as antibiotics, bisphenol A, and 1,4-dioxane in pure conditions, e.g. dilution in pure water [18–20]. However, the results are not representative of real natural water containing substantial amounts of humic substances. Therefore, here we tested the removal of humic acids using persulfate combined with corn stalk biochar. We used both pure aqueous solutions and real water from the Yangtze River. We monitored fluorescence, UV and total organic carbon (TOC) to follow changes in composition and removal of humic substances, respectively. We also carried out quench experiments to identify involved radical to infer possible mechanisms.

Table 1
The removal efficiency of different biochar combined with persulfate.

Material	Optimal experiment terms	Pollutant	Removal rate	Ref.
Egg-derived biochar (ES-biochar)	[ES-800] = 0.167 g/L, [PS] = 1 g/L, [2,4-DCP] = 100 mg/L, pH = 6.	2,4-Dichlorophenol (2,4-DCP)	More than 90% (ES-800, 120 min)	[15]
Corn stalk biochar (CBC)	NOR = 10 mg/L, CBC dosage = 0.8 g/L, PS/NOR molar ratio = 120/1.	Norfloxacin (NOR)	94.21% (BC-500, 300 min)	[14]
Mn doped magnetic biochar (MMBC)	[MMBC] = 0.2 g/L, [PS] = 8 mM, [TC] = 20 mg/L, [pH] = 3, [Temp] = 298 K.	Tetracycline (TC)	93% (MMBC-900, 180 min)	[42]
Sludge-derived biochar (SBC)	pH 7.2, SBC dosage of 1.0 g/L and PMS concentration of 0.8 mM at 25 °C.	Triclosan (TCS)	99.2% (240 min)	[56]
Pine needle biochar	[PMS] = 8.0 mM, [1,4-dioxane] = 20.0Mm, [biochar] = 1.0 g/L, T = 25 °C, pH = 6.5.	1,4-Dioxane	84.2% (BC-800, 250 min)	[57]
Lychee branch biochar	[PS] = 8 mM, [BPA] = 5 mg/L, T = 25 °C, BC = 1 g/L, pH = 7.	Bisphenol A (BPA)	82.68% (BC-600, 120 min)	[33]
Sludge-derived biochar (SDBC)	[PDS] = 1.5 mM, [SMX] = 40 μM, SDBC dosage = 2.0 g/L, pH ≈ 5.0, T = 25 °C.	Sulfamethoxazole (SMX)	94.6% (SDBC-700, 180 min)	[58]
Magnetic rape straw biochar (MRSB)	1 g/L MRSB, 8 mM PS, initial pH 2.99–11.01, 25 °C.	Tetracycline hydrochloride (TC)	More than 88% (MRSB-400, 120 min)	[16]
Fe/Mn modified sludge-derived biochar (Fe/MnBC)	[RB19] = 1000 mg/L, pH = 7, [PS] = 8 mmol/L, [Fe/MnBC] = 0.4 g/L.	Reactive blue 19 (RB19)	98.33% (Fe/MnBC-600, 18 h)	[17]
Sawdust biochar (SBC)	[PS] = 9 mmol/L, [SBC] = 1.5 g/L, [AO7] = 50 mg/L, pH 2–10.	Acid orange 7 (AO7)	Over 90% (SBC-700, 180 min)	[59]

2. Materials and methods

2.1. Reagents

Humic acids (HA), hydrochloric acid (HCl), sodium hydroxide (NaOH), sodium persulfate (PS, $Na_2S_2O_8$), tert-butyl-alcohol (TBA) and methanol (MeOH) were purchased from Sinopharm Chemical Regent Co. Ltd., Shanghai, China. All chemicals were of analytical grade and were used as received. Unless otherwise specified, deionized water was used in all experiments.

2.2. Preparation and modification of corn stalk biochar

Corn stalks were collected in autumn from a rural area in Anhui, China. Before use, straws were cut to about 100 mesh, cleaned and dried at 60 °C. Dried straw powder was placed in a box furnace and the temperature was raised to 400 °C, 600 °C, 700 °C and 900 °C under dinitrogen atmosphere at a heating rate of 5 °C/min, then kept for 180 min at corresponding temperature. The corn stalk samples were taken out after the pyrolysis and then soaked in 10% (w/w) HCl solution for 12 h. Subsequently, the corn stalk samples were washed with deionized water to neutral pH and dried at 60 °C to obtain the corn stalk biochar. The particle size range of biochar used in the experiment was 0.5–1 mm.

2.3. Removal of humic acids in pure conditions

To explore the effect of different factors on humic acids (HA) removal, a batch experiment in pure water was carried out. A measured volume of stock humic solution was mixed with the deionized water to reach the desired HA concentration. The desired amount of persulfate (PS) and biochar was immediately added to a conical flask, which filled with 100 mL of HA solution. Then 5 mL of the solution was collected from the flask placed on a constant temperature shaker (25 °C, 200 rpm) and filtered with a membrane (0.45 μm) at a certain time interval to monitor the removal of humic acid. The effects of biochar dosage of 0.1–0.9 g/L, initial pH of 5.0–9.0, PS concentration of 0.2–2 mM and initial HA concentration of 5–15 mg/L on HA removal were explored. The UV spectrophotometer was used to analyze the concentration of HA at 254 nm. HCl or NaOH (0.1 M) was used to adjust the initial pH of the solution.

To further identify the presence of free radicals in the reaction, a quenching experiment was carried out. Specifically, tert-butyl-alcohol (TBA) and methanol (MeOH) were used to quench •OH and SO_4^{-}•, respectively. All experiments were carried out for three times.

2.4. Removal of organic matter from river water and regeneration tests

To explore the application of biochar combined with persulfate in real water, water samples from the inlet of a reservoir in the Yangtze River were collected to a 2.5 L stainless steel column sampler and put into a collection bottle made of highly density polyethylene. After sampling, the water samples were immediately taken back to the laboratory for storage in a 4 °C refrigerator prior to use. Meanwhile, regeneration tests were used to judge reusability by collecting the used biochar through filtration and dried it in an oven at 60 °C for next use.

2.5. Data analysis and processing

The morphological characteristics, crystal structure, surface functional groups, surface pore distribution of biochar were analyzed by scanning electron microscopy (SEM, S4800, Hitachi, Japan), X-ray diffraction (XRD, Rigaku Ultima IV, Japan), Fourier transform infrared spectroscopy (FT-IR, Bruker/tensor 27, Germany) and Brunauer-Emmett-Teller (BET, Autosorb iQ2-up, Quantachrome, America), respectively. And the zero point of charge pH_{ZPC} of the biochar was determined by the salt drop method.

HA removal was determined by a UV–vis spectrophotometer (UV-2600, SHIMADZU, China) at 254 nm (UV_{254}). The HA removal efficiency R_{HA} (%) was calculated using Eq. (1).

$$R_{HA}\ (\%) = C_t/C_0 \tag{1}$$

where C_0 and C_t represent HA concentration (mg/L) at the initial and time t, respectively. R_{HA} (%) refers to the removal rate (%) of HA.

Total organic carbon (TOC) was measured by a TOC analyzer (Muliti N/C 3100, Jena Analytical Instrument Co, Ltd), with Eq. (2) to calculate the removal rate:

$$R_{TOC} = TOC_t/TOC_0 \tag{2}$$

where TOC_0 and TOC_t represent TOC concentration (mg/L) at the start time and time *t*, respectively.

EEMs of samples were determined by a fluorescence spectrophotometer (F-7000, Hitachi, Japan) to study the composition

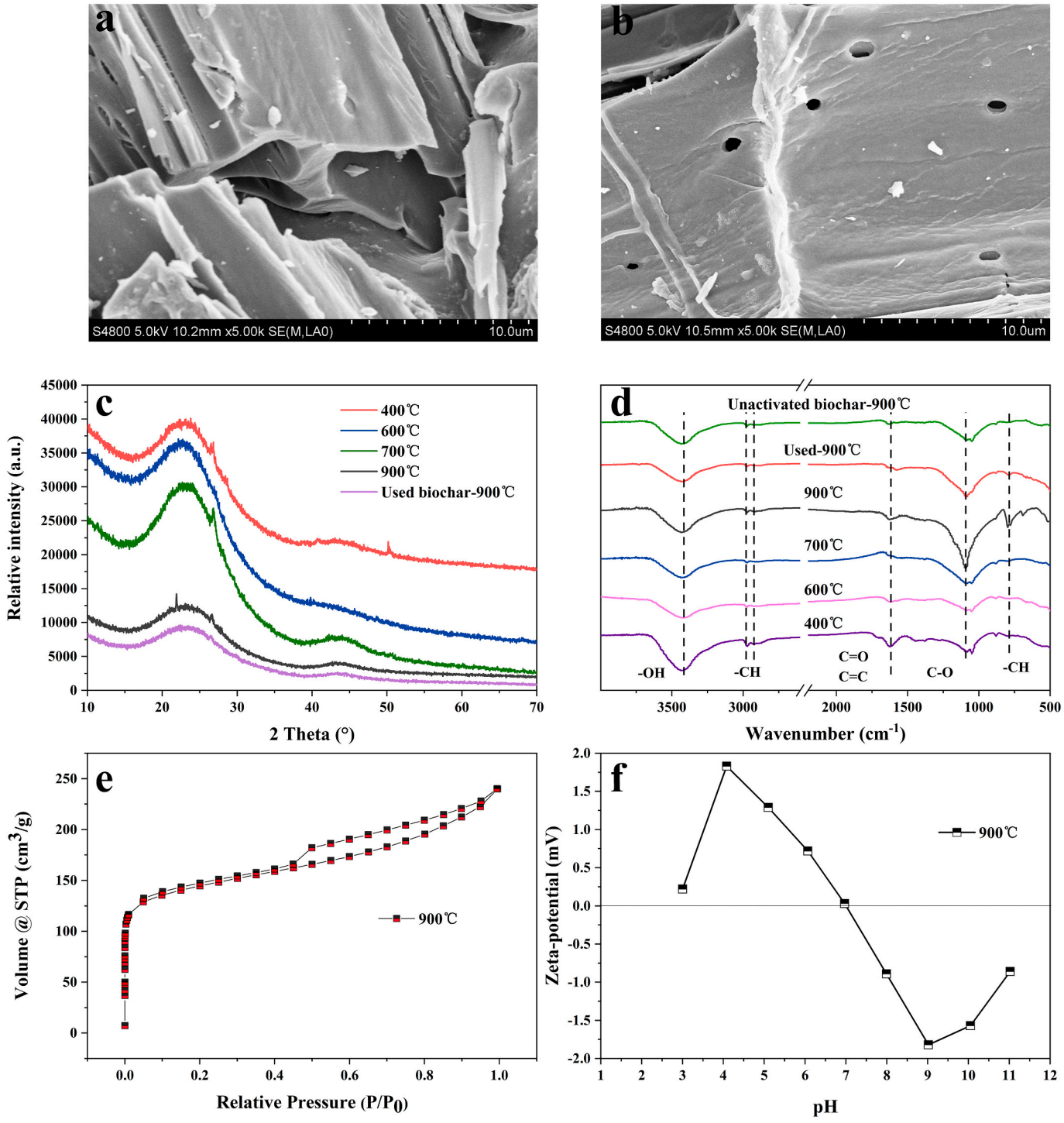

Fig. 1. Scanning electron microscopy (SEM) images of biochar-900 °C(a) raw biochar, (b) biochar after HCl treatment; (c) X-Ray diffraction (XRD) and (d) Fourier transform infrared spectroscopy (FTIR) of biochar prepared at 400 °C, 600 °C, 700 °C and 900 °C after HCl treatment, in raw form ('Unactivated') and after three successive treatments ('Used') of a solution of 5 mg/L humic acids (HA) and 1 mM persulfate at pH 8.0 with 0.5 g/L biochar; (e) nitrogen adsorption-desorption isotherms and (f) surface zeta potential of biochar-900 °C.

characteristics of HA by scanning the emission spectra from 250 nm to 550 nm at 5 nm wavelength increments and the excitation wavelengths from 200 nm to 500 nm at 5 nm wavelength increments. The scanning speed was set at 12,000 nm/min. The pH values were determined using a pH meter (PXSJ-226, LEICI, China).

3. Results and discussion

3.1. Characterization of corn stalk biochar

The morphology of biochar from corn stalks was analyzed by scanning electron microscopy (SEM). Fig. S1 presents biochar produced at different pyrolysis temperatures after soaking in HCl. The shape of biochar is hollow strip structure. The pore structure is being developed with the pyrolysis temperature increasing. After HCl treatment, more pore structures appear on the surface of biochar prepared at 900 °C (Fig. 1a and b). Previous studies have reported that post-treatment of biochar can improve characteristics of biochar more gently [21,22]. This morphology is typical of a good adsorbent and catalyst [23]. We thus used the HCl-treated biochar for next experiments.

Furthermore, Fig. 1c exhibits X-ray diffraction (XRD) patterns of biochar. Two broad diffraction peaks at around 23° and 43°are indexed to (002) C planes and (100) C planes respectively, suggesting thermolytic transformation of corn stalk to amorphous carbon [24]. After carbonization of the biomass to 900 °C, two board peaks became wider and weaker, implying the decomposition of partial amorphous carbon.

FTIR analysis of biochar (Fig. 1d) shows a peak at around 3410 cm^{-1}, which is assigned to the vibration of O—H in carboxyl and phenol [25]. The appearance of peaks at 2969 cm^{-1} and 2884 cm^{-1} are due to the stretching of the aliphatic functional group C—H [26]. The existence of the elongation of C═O and C═C functional groups might be proved by the peak around 1606 cm^{-1} [27]. The distinct peak at about 1081 cm^{-1} corresponds to the C—O vibration of carboxyl and phenol [28]. An aromatic C—H bending deformation is observed at 760 cm^{-1} and 820 cm^{-1} [29]. We observed that the oxygen-contained functional groups decreased with the increase of pyrolysis temperature from 400 °C to 900 °C, especially for O—H around 3410 cm^{-1}. For biochar produced at 900 °C, after HCl modification, the intensities of the functional groups such as -OH, C—O and C=O/C=C increased significantly. After reaction, the intensity of peaks at 3410 cm^{-1}, 1606 cm^{-1} and 1081 cm^{-1} decreased. Pan et al. summarized recent literature and found that the O-containing functional groups including -OH, -C=O-, -COOH on the surface of biochar are important active sites for activating persulfate [30]. Based on the above results, we inferred that the oxygen-containing functional groups on the surface of biochar might be involved in the activation of persulfate.

The adsorption-desorption curve of corn biochar prepared at 900 °C shows a type-IV adsorption/desorption isotherm (Fig. 1e), suggesting the existence of mesoporous structure in the biochar [19]. When the pyrolysis temperature increased from 400 °C to 900 °C, the specific surface area and total pore volume of biochar was 3.05 m^2/g, 4.42 m^2/g, 22 m^2/g, 459.260 m^2/g, 0.01 cm^3/g, 0.015 cm^3/g, 0.026 cm^3/g and 0.37 cm^3/g, respectively. The increase of pyrolysis temperature promoted the increase of specific surface area and the total pore volume due to the gradual transformation of corn straw into porous carbon structure and the partial decomposition of amorphous carbon, accompanied by the loss of volatile substances [31,32]. Analysis of surface-charge properties show that the zeta potential of biochar-900 °C is about 7.0, indicating a pH neutral surface (Fig. 1f).

Fig. 2 shows the biochar produced at different pyrolysis temperature and used to combine with persulfate to remove humic acid. With the increase of pyrolysis temperature, the ability of biochar combined with persulfate to remove humic acid increased. When the carbonization temperature reached 900 °C, the removal rate increased significantly to 89% within 120 min. Therefore, biochar pyrolyzed at 900 °C was used to combine persulfate for subsequent experiments.

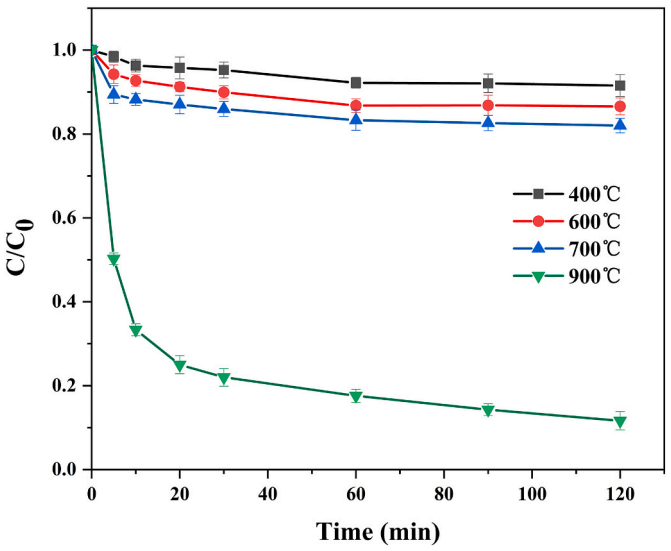

Fig. 2. Humic acid removal of biochar at different pyrolysis temperatures in the condition of 5 mg/L humic acids (HA) and 1 mM persulfate at pH 8.0 with 0.5 g/L biochar.

3.2. Removal of HAs by adsorption and oxidation

We compared the removal of humic acids in water using persulfate, corn stalk biochar, and biochar combined with persulfate by determining the concentration of humic acids in the solution (Fig. 3a). With persulfate alone, the removal rate of humic acids was very low, of less than 5%, indicating that the oxidation activity of persulfate alone at 25 °C is very weak, in agreement with the results of [33]. With corn stalk biochar at 0.5 g/L, 57% of humic acids were removed at pH 8 after 180 min, indicating the high adsorption capacity of biochar. With corn stalk biochar combined with persulfate, humic acids removal reached 88%, indicating the synergic effect between biochar and persulfate.

We further assessed the removal of humic acids by measuring the total organic carbon (TOC) of the solution (Fig. 3b). Overall, our findings showed that humic acid removal was much higher with combined biochar and persulfate treatment. TOC removal was low with persulfate alone, of 5.1%, implying the concurrence of oxidation, with corn stalk biochar removal increased to 45.9% by adsorption. Application of both biochar and persulfate brought about HA removal of 71.9%, which was much higher than the sum of previous runs (51%). The results implied the occurrence of other mechanisms such as activation of persulfate by humic acids and biochar [33,34], thus improved adsorption on biochar surface following the reaction of biochar with persulfate [35].

We analyzed the composition of humic acid solutions treated by persulfate, biochar and biochar combined with persulfate by three-dimensional fluorescence excitation-emission matrix (3D-EEM) (Fig. 3c, d, e and f). Fluorescence spectra can be divided into four sectors (Table S1), consisting of humic acids, fulvic acids, soluble microbial products (SMP) and protein-like material such as tryptophan and tyrosine [36]. Results of the initial humic solution showed three main spots corresponding to humic acids, fulvic acids and protein-like materials. Dosing persulfate alone reduced the fluorescence intensity slightly, which strengthened the minor contribution of oxidation of previous results. In contrast, adding either biochar or biochar and persulfate together induced a disappearance of humic and fulvic acid spots, in agreement with the high removal results in Fig. 3a and b.

3.3. Effects of concentrations and pH on the removal of HAs in pure conditions

Fig. 4a demonstrated that humic acids removal increased from

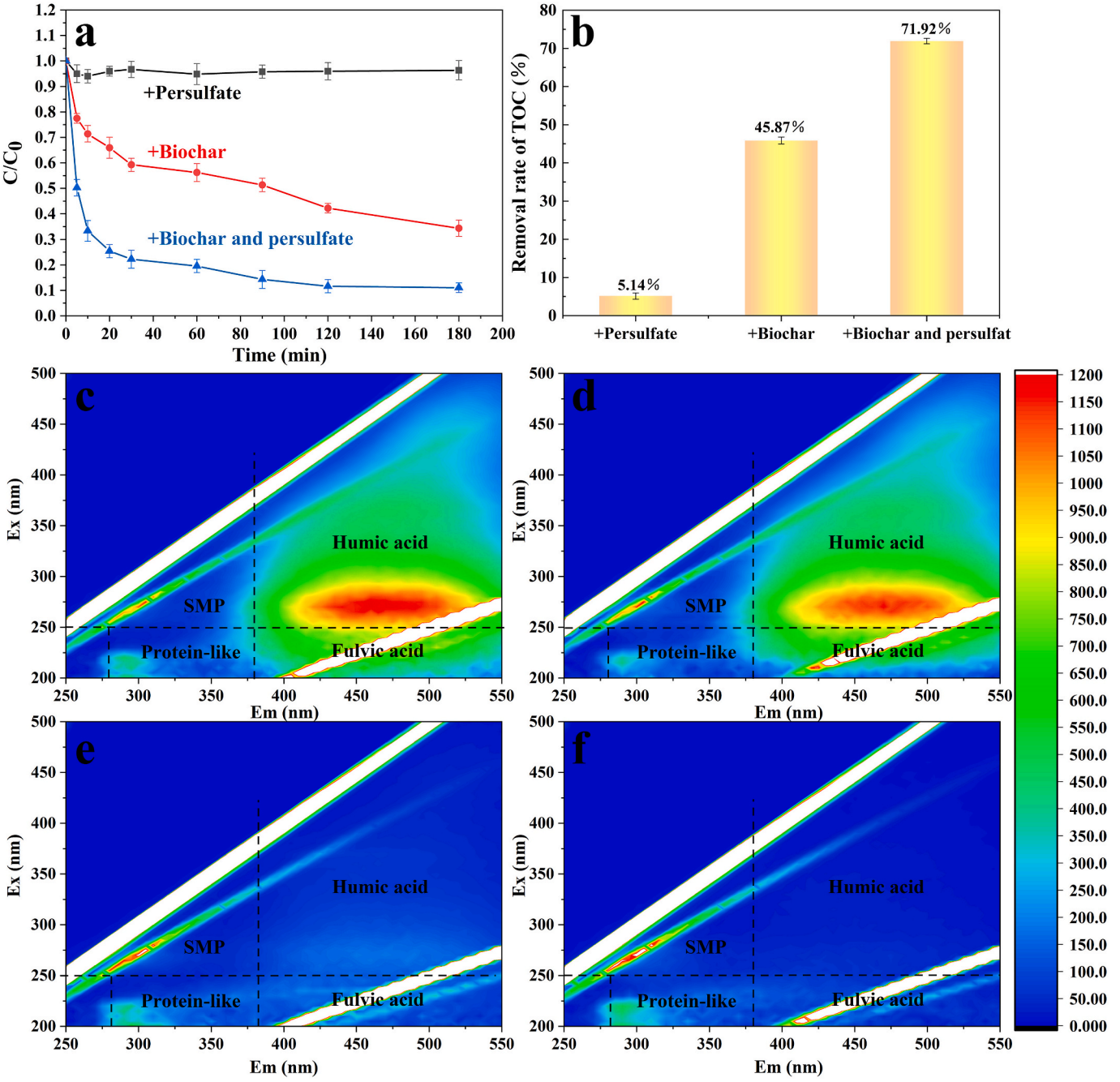

Fig. 3. a) Relative concentration of humic acids and b) aqueous total organic carbon (TOC) removal after 180 min, in solutions containing persulfate (PS), biochar or biochar and persulfate. Fluorescence spectra of solutions containing c) initial humic acids, d) humic acids and persulfate, e) humic acids and biochar, f) humic acids, biochar and persulfate after 180 min of reaction.

47.34% to 86.70% with biochar concentration from 0.1 g/L to 0.9 g/L after 120 min. This trend was probably due to the increase in the number of active sites according to [14]. When the dosage was above 0.5 g-biochar/L, the increase of humic acid removal was not obvious and the difference of the final removal rate was very small. In terms of cost, 0.5 g/L was used as the dosage of biochar in the subsequent tests.

Fig. 4b demonstrated that humic removal increased from 70.11% at 0.2 mM persulfate to 85.06% at 1 mM persulfate, then slightly decreased to 80.46% at 2 mM persulfate after 180 min. The increase was explained by the generation of more free radicals that react with humic acids [5]. The following decrease was due to the limited biochar active sites and the quenching reaction with an excess of $SO_4^{-\bullet}$ (Eq. (3)) [37]. Moreover, excess free radicals can react with persulfate and inactivate (Eq. (4)) [38], thus suppressing the removal of humic acids. In addition, persulfate may decompose during the reaction according to [39]. In summary, persulfate should be controlled within an appropriate range. Therefore, 1 mM was used as the PS concentration selected in the subsequent experiments.

$$SO_4^{-} + SO_4^{-} \rightarrow S_2O_8^{2-} \quad (3)$$

$$S_2O_8^{2-} + SO_4^{-} \rightarrow SO_4^{2-} + S_2O_8^{-} \quad (4)$$

Fig. 4c showed that pH variations from 5.0 to 9.0 had only minor effect on the removal of humic acids, which reached 90.7% at pH 5.0 and 90.1% at pH 9.0 within 180 min. Those trends were explained by the following processes: persulfate treatment induced the release of H^+, thus

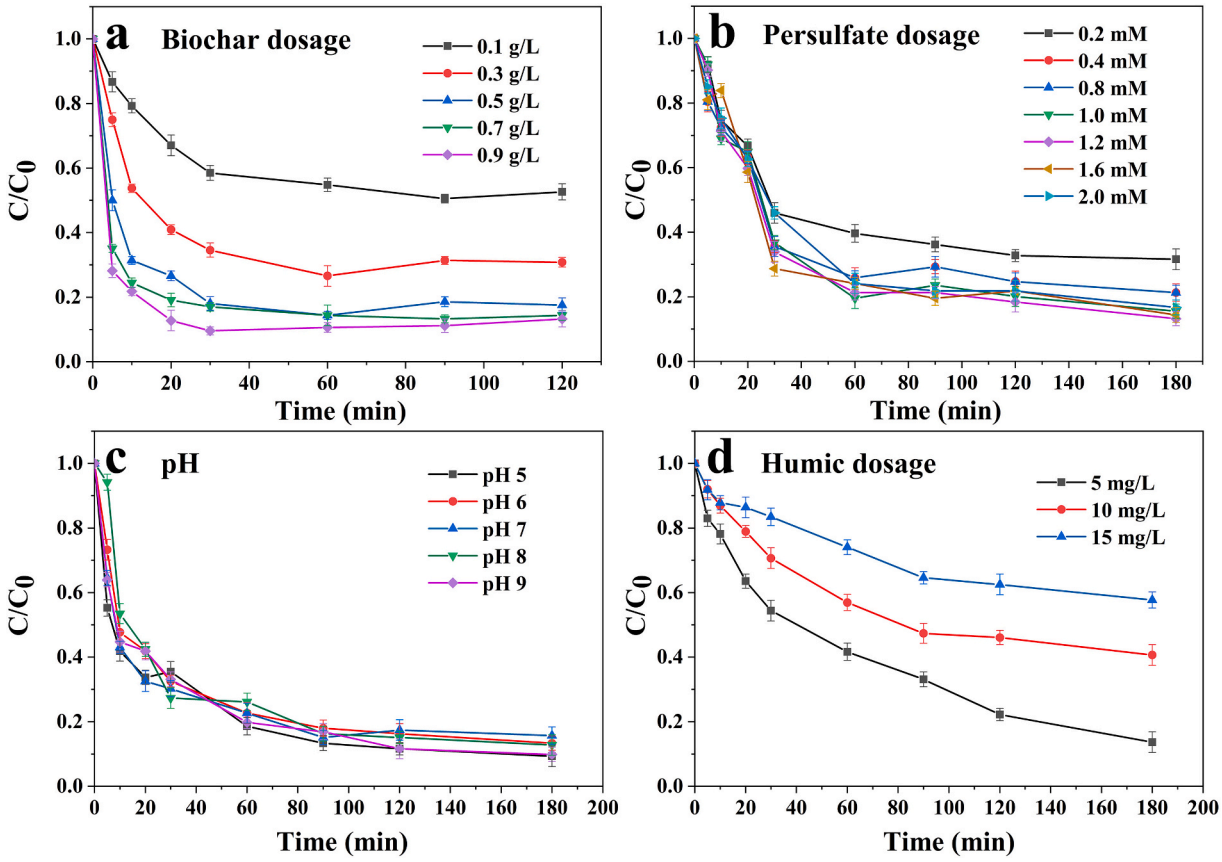

Fig. 4. Effects of a) biochar dosage, b) persulfate concentration, c) pH, and d) humic acids concentration on the removal of humic acids. Conditions: a) 5 mg/L humic acids, 1 mM persulfate, pH 8.0; b) 5 mg/L humic acids, 0.5 g/L biochar, pH 8.0; c) 5 mg/L humic acids, 0.5 g/L biochar, 1 mM persulfate, d) 0.5 g/L biochar, 1 mM persulfate, pH 8.0.

causing pH drop first, favoring the adsorption of humic acid negatively-charged functions and $S_2O_8^{2-}$. Humic acids were less charged due to the increase of H^+, and were easily adsorbed in turn [11]. Fig. 4d showed that removal rate of humic acid increased with its initial concentration. This was explained by an excess of humic acids versus active reaction sites. Overall, our findings showed that humic acid removal increased with biochar and persulfate concentration up to a limiting threshold, and that removal was little affected by pH. The final removal rate of HA according to the effect of different key factors was listed in (Tables S2, S3 and S4).

3.4. Regeneration of used biochar and treatment of river water with biochar and persulfate

We tested the efficiency of biochar in three consecutive treatments of humic acids with persulfate (Fig. S2). Results showed that humic acid removal dropped from 87.21%at the first treatment to 39.14% at the second treatment and 28.10% at the third treatment after 180 min, revealing the poor recyclability of biochar. This was supported by microscopic analysis that reveals pore destruction and decreasing pore volume (Fig. S3). The specific surface area and the total pore volume of the biochar after reaction decreased from 459.260 m^2/g to 247.992 m^2/g and from 0.372 cm^3/g to 0.256 cm^3/g, respectively. X-ray diffraction also showed that peaks at 23° and 43.0° are weakened (Fig. 1c). These observations were similar to surface coverage by organics observed previously on the surface of biochar [40]. We also tested the stability of biochar, and we found that humic removal efficiency was still good after 6 months of storage (Fig. S2). Overall, used biochar is poorly recyclable, but unused biochar is stable upon storage.

In order to explore the practical application of biochar, we applied the system of persulfate combined with biochar to the actual water body. The initial concentration of total organic carbon in the solution, of 2.43 mg/L, decreased by 69.7% after synergistic treatment of river water with biochar and persulfate (Fig. S4). 80.4% removal efficiency of UV_{254} could be achieved after 180 min. Fluorescence analysis also revealed an almost complete disappearance of the four organic spots (Fig. 5). Our findings evidenced the good application of biochar and persulfate to clean river water containing moderate organic levels. The characteristics of the real water samples were listed in Table 2.

3.5. Mechanism of humic acid removal by a combination of persulfate and biochar

Previous researches have shown that $SO_4^{-\bullet}$ and •OH are the main free radicals reacting with organic substances [16,17,41]. As common quenchers, MeOH is often used as a quencher for both •OH and $SO_4^{-\bullet}$, whereas TBA is used to quench •OH because TBA reacts more efficiently with •OH than with $SO_4^{-\bullet}$ [42–44]. Our results showed that adding TBA decreased the removal of humic acids by 12.8% for a TBA/persulfate molar ratio of 500/1 and by 15.6% for 1000/1 (Fig. 6) after 180 min. By contrast, MeOH addition showed only a minor quenching effect of 4.8% for a 1000/1 molar ratio of MeOH/persulfate within the same time. Since TBA has much higher affinity for •OH than MeOH [45], our findings suggested that •OH are the dominant free radicals. This hypothesis was supported by similar trends observed in previous reports [13,46,47]. Overall, the results suggested that both •OH and, to a lesser extent, $SO_4^{-\bullet}$, were involved in the reactions.

Biochar played an important role in the whole reaction, participating in the adsorption and oxidation process in the persulfate and biochar system. Pyrolysis temperature can significantly change the composition,

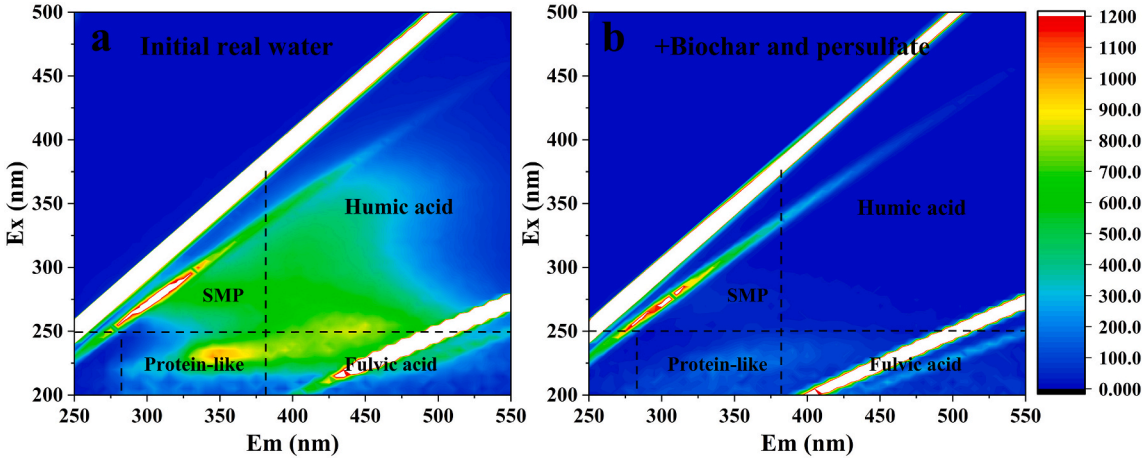

Fig. 5. Fluorescence spectra of river water before (a) and after treatment with 0.5 g/L biochar and 1 mM persulfate (b) of 180 min.

Table 2
The characteristics of the real water samples.

Parameters	Average value
pH	8.48
Conductivity (μS/cm)	285
Total organic carbon (TOC) (mg/L)	2.43
Dissolved oxygen (DO) (mg/L)	8.87
Oxidation-reduction potential (mV)	18.8
Total dissolved solids (TDS) (mg/L)	216.8

structure and functional groups of biochar [48]. With the increase of pyrolysis temperature from 400 °C to 900 °C, biochar generated more pore structure and bigger specific surface area, providing more active sites for the removal of organic matter in the process of adsorption and oxidation [30,49]. Previous studies have reported that high specific surface area and appropriate pore structure can provide channels for material dispersion and improve mass transfer [50,51]. After HCl modification, the impurities on the surface of biochar were better removed, and more oxygen-containing functional groups were introduced, improving the adsorption and catalytic properties of biochar.

On the one hand, the adsorption of biochar was significant, which can perform physical adsorption, e.g. encapsulation and electrostatic interactions, or chemical adsorption, e.g. by H and covalent bonds occurred on the surface of biochars to adsorb humic acid and persulfate [52,53]. On the other hand, the inhibitory effect of alcohols on the removal rate of the reaction suggested that $SO_4^{-\bullet}$ and $^{\bullet}OH$ were involved in the reaction process. XRD analysis of biochar showed the presence of sp^2 carbons at 43.0° (Fig. 1c), facilitating the transfer of electrons [54]. FTIR analysis of biochar showed the presence of O-bearing groups. According to reports, the oxygen-containing functional groups contained in biochar can be used as electron transfer media to promote the generation of free radicals [55].

Therefore, we proposed the main mechanism for the synergistic removal of HA in water with biochar and persulfate (Fig. 7). Firstly, humic acids and persulfate migrate from the liquid phase to the biochar surface and are adsorbed. The oxygen-containing functional groups on the surface of biochar act as the medium of electron transfer, so that persulfate is provided with electrons, leading to the breakage of O—O bond in persulfate; $SO_4^{-\bullet}$ is produced (Eqs. (5), (6)), which continues to react in solution to generate other kinds of active free radicals to degrade humic acid and its intermediate products (Eqs. (7), (8)) [17].

$$\text{Biochar}-\text{COOH}+S_2O_8^{2-}\rightarrow SO_4^{-\bullet}+HSO_4^{-}+\text{Biochar}-\text{COO} \quad (5)$$

$$\text{Biochar}-\text{OH}+S_2O_8^{2-}\rightarrow SO_4^{-\bullet}+HSO_4^{-}+\text{Biochar}-\text{O} \quad (6)$$

$$SO_4^{-\bullet}+H_2O\rightarrow SO_4^{2-}+OH \quad (7)$$

$$SO_4^{-}+OH^{-}\rightarrow SO_4^{2-}+OH+H^{+} \quad (8)$$

4. Conclusion

In summary, this work prepared a high-temperature corn stalk biochar that was easy to obtain and synthesize, which had relatively large surface area and abundant oxygen-containing functional groups.

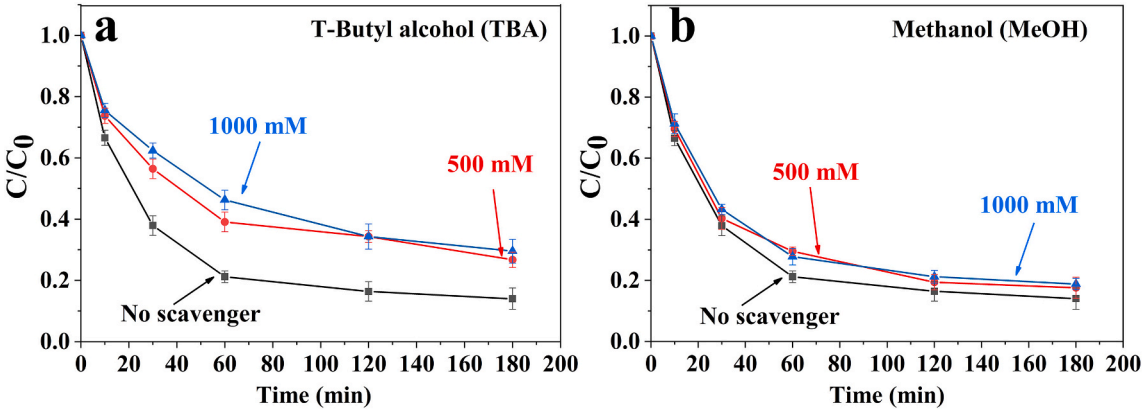

Fig. 6. Relative concentration of humic acids after addition of radical scavengers tert-but alcohol (TBA) (a) and methanol (MeOH) (b) in reactions of humic acids with biochar and persulfate.

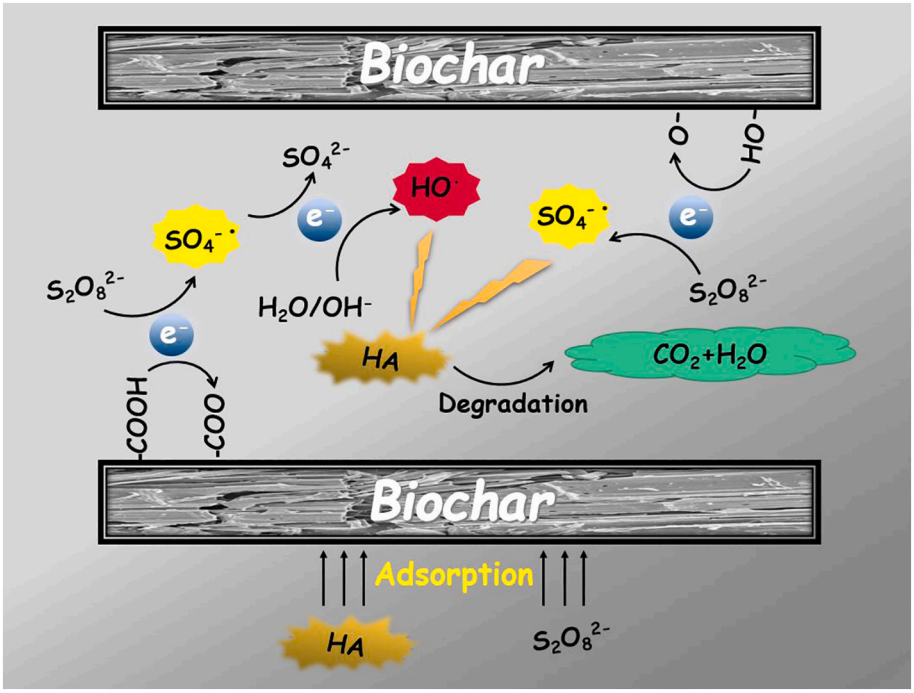

Fig. 7. Proposed main mechanism of humic acid removal in solutions containing biochar and persulfate.

Reaction of biochar with humic acids and persulfate in pure conditions induced up to 84.3% of humic acid removal at pH 5.0–9.0. Batch experiments showed that within a certain range, the removal of humic acid increased with the increase of persulfate and biochar. Reaction with river water confirmed the efficiency of this method for real applications, including good removal of fluorescent components and 69.7% removal of TOC and 80.4% removal of UV_{254}. Biochar displayed good storage capacity, but was poorly recyclable. Humic acid removal was explained by a tentative mechanism involving mainly adsorption and oxidation by of •OH and SO_4^{-}•, which could be further proved by radical quenching experiment, FTIR, SEM and XRD. The oxygen-containing functional groups -OH and -COOH on the surface of biochar played an important role in the reaction.

Declaration of competing interest

The authors have declared no conflict of interest.

Acknowledgments

We gratefully acknowledged the co-funding of this work by the National Natural Science Foundation of China (No. 52070130) and the Shuguang Project of Shanghai (Education and Scientific Research Project of Shanghai, 18SG45).

Appendix A. Supplementary data

Supplementary data to this article can be found online at https://doi.org/10.1016/j.jwpe.2021.102428.

References

[1] S. Dou, J. Shan, X. Song, R. Cao, M. Wu, C. Li, S. Guan, Are humic substances soil microbial residues or unique synthesized compounds? A perspective on their distinctiveness, Pedosphere 30 (2020) 159–167.
[2] Q. Du, S. Zhang, J. Song, Y. Zhao, F. Yang, Activation of porous magnetized biochar by artificial humic acid for effective removal of lead ions, J. Hazard. Mater. 389 (2020).
[3] É. Lichtfouse, Temporal pools of individual organic substances in soil, Analusis 27 (1999) 442–446.
[4] M. Schnitzer, Chapter 1 humic substances: chemistry and reactions, in: M. Schnitzer, S.U. Khan (Eds.), Developments in Soil Science, Elsevier, 1978.
[5] W. Zhang, Y. He, C. Li, X. Hu, S. Yang, X. You, W. Liang, Persulfate activation using Co/AC particle electrodes and synergistic effects on humic acid degradation, Appl. Catal. B Environ. (2021) 285.
[6] P. Herzsprung, W. von Tümpling, N. Hertkorn, M. Harir, O. Büttner, J. Bravidor, K. Friese, P. Schmitt-Kopplin, Variations of DOM quality in inflows of a drinking water reservoir: linking of van Krevelen diagrams with EEMF spectra by rank correlation, Environ. Sci. Technol. 46 (2012) 5511–5518.
[7] L. Wang, C. Han, M.N. Nadagouda, D.D. Dionysiou, An innovative zinc oxide-coated zeolite adsorbent for removal of humic acid, J. Hazard. Mater. 313 (2016) 283–290.
[8] A. Imyim, E. Prapalimrungsi, Humic acids removal from water by aminopropyl functionalized rice husk ash, J. Hazard. Mater. 184 (2010) 775–781.
[9] Y. Ai, C. Zhao, L. Sun, X. Wang, L. Liang, Coagulation mechanisms of humic acid in metal ions solution under different pH conditions: a molecular dynamics simulation, Sci. Total Environ. 702 (2020), 135072.
[10] L.-L. Hwang, J.-C. Chen, M.-Y. Wey, The properties and filtration efficiency of activated carbon polymer composite membranes for the removal of humic acid, Desalination 313 (2013) 166–175.
[11] H. Yang, B. Luo, S. Lei, Y. Wang, J. Sun, Z. Zhou, Y. Zhang, S. Xia, Enhanced humic acid degradation by Fe3O4/ultrasound-activated peroxymonosulfate: synergy index, non-radical effect and mechanism, Sep. Purif. Technol. 264 (2021), 118466.
[12] N. Yousefi, S. Pourfadakari, S. Esmaeili, A.A. Babaei, Mineralization of high saline petrochemical wastewater using Sonoelectro-activated persulfate: degradation mechanisms and reaction kinetics, Microchem. J. 147 (2019) 1075–1082.
[13] A. Lykoudi, Z. Frontistis, J. Vakros, I.D. Manariotis, D. Mantzavinos, Degradation of sulfamethoxazole with persulfate using spent coffee grounds biochar as activator, J. Environ. Manag. 271 (2020), 111022.
[14] B. Wang, Y.N. Li, L. Wang, Metal-free activation of persulfates by corn stalk biochar for the degradation of antibiotic norfloxacin: activation factors and degradation mechanism, Chemosphere 237 (2019), 124454.
[15] H. Liu, Y. Liu, L. Tang, J. Wang, J. Yu, H. Zhang, M. Yu, J. Zou, Q. Xie, Egg shell biochar-based green catalysts for the removal of organic pollutants by activating persulfate, Sci. Total Environ. 745 (2020), 141095.
[16] H. Huang, T. Guo, K. Wang, Y. Li, G. Zhang, Efficient activation of persulfate by a magnetic recyclable rape straw biochar catalyst for the degradation of tetracycline hydrochloride in water, Sci. Total Environ. 758 (2021), 143957.
[17] Y. Qiu, Q. Zhang, Z. Wang, B. Gao, Z. Fan, M. Li, H. Hao, X. Wei, M. Zhong, Degradation of anthraquinone dye reactive blue 19 using persulfate activated with Fe/Mn modified biochar: radical/non-radical mechanisms and fixed-bed reactor study, Sci. Total Environ. 758 (2021), 143584.
[18] D. Ouyang, J. Yan, L. Qian, Y. Chen, L. Han, A. Su, W. Zhang, H. Ni, M. Chen, Degradation of 1,4-dioxane by biochar supported nano magnetite particles activating persulfate, Chemosphere 184 (2017) 609–617.
[19] B. Shen, Y. Liu, S. Liu, X. Tan, P. Zhang, L. Du, J. Wen, Catalytic degradation of sulfamethoxazole by persulfate activated with magnetic graphitized biochar: multiple mechanisms and variables effects, Process. Saf. Environ. Prot. 144 (2020) 143–157.

[20] L. Zhao, Y. Ji, D. Kong, J. Lu, Q. Zhou, X. Yin, Simultaneous removal of bisphenol A and phosphate in zero-valent iron activated persulfate oxidation process, Chem. Eng. J. 303 (2016) 458–466.
[21] C. Wang, R. Huang, R. Sun, J. Yang, M. Sillanpää, A review on persulfates activation by functional biochar for organic contaminants removal: synthesis, characterizations, radical determination, and mechanism, J. Environ. Chem. Eng. 9 (2021).
[22] J. Yu, L. Tang, Y. Pang, G. Zeng, J. Wang, Y. Deng, Y. Liu, H. Feng, S. Chen, X. Ren, Magnetic nitrogen-doped sludge-derived biochar catalysts for persulfate activation: internal electron transfer mechanism, Chem. Eng. J. 364 (2019) 146–159.
[23] J. Wang, S. Wang, Preparation, modification and environmental application of biochar: a review, J. Clean. Prod. 227 (2019) 1002–1022.
[24] W.-D. Oh, G. Lisak, R.D. Webster, Y.-N. Liang, A. Veksha, A. Giannis, J.G.S. Moo, J.-W. Lim, T.-T. Lim, Insights into the thermolytic transformation of lignocellulosic biomass waste to redox-active carbocatalyst: durability of surface active sites, Appl. Catal. B Environ. 233 (2018) 120–129.
[25] K. Luo, Q. Yang, Y. Pang, D. Wang, X. Li, M. Lei, Q. Huang, Unveiling the mechanism of biochar-activated hydrogen peroxide on the degradation of ciprofloxacin, Chem. Eng. J. 374 (2019) 520–530.
[26] X. Zhu, Y. Liu, F. Qian, C. Zhou, S. Zhang, J. Chen, Preparation of magnetic porous carbon from waste hydrochar by simultaneous activation and magnetization for tetracycline removal, Bioresour. Technol. 154 (2014) 209–214.
[27] D.D. Warnock, J. Lehmann, T.W. Kuyper, M.C. Rillig, Mycorrhizal responses to biochar in soil – concepts and mechanisms, Plant Soil 300 (2007) 9–20.
[28] J. Zhang, Q. Wang, Sustainable mechanisms of biochar derived from brewers' spent grain and sewage sludge for ammonia–nitrogen capture, J. Clean. Prod. 112 (2016) 3927–3934.
[29] X. Dong, L.Q. Ma, Y. Zhu, Y. Li, B. Gu, Mechanistic investigation of mercury sorption by Brazilian pepper biochars of different pyrolytic temperatures based on X-ray photoelectron spectroscopy and flow calorimetry, Environ. Sci. Technol. 47 (2013) 12156–12164.
[30] X. Pan, Z. Gu, W. Chen, Q. Li, Preparation of biochar and biochar composites and their application in a Fenton-like process for wastewater decontamination: a review, Sci. Total Environ. 754 (2021), 142104.
[31] X. Wang, W. Zhou, G. Liang, D. Song, X. Zhang, Characteristics of maize biochar with different pyrolysis temperatures and its effects on organic carbon, nitrogen and enzymatic activities after addition to fluvo-aquic soil, Sci. Total Environ. 538 (2015) 137–144.
[32] L. Zhao, W. Zheng, X. Cao, Distribution and evolution of organic matter phases during biochar formation and their importance in carbon loss and pore structure, Chem. Eng. J. 250 (2014) 240–247.
[33] J. Liu, S. Jiang, D. Chen, G. Dai, D. Wei, Y. Shu, Activation of persulfate with biochar for degradation of bisphenol A in soil, Chem. Eng. J. 381 (2020), 122637.
[34] G. Fang, J. Gao, D.D. Dionysiou, C. Liu, D. Zhou, Activation of persulfate by quinones: free radical reactions and implication for the degradation of PCBs, Environ. Sci. Technol. 47 (2013) 4605–4611.
[35] Q. Fan, J. Sun, L. Chu, L. Cui, G. Quan, J. Yan, Q. Hussain, M. Iqbal, Effects of chemical oxidation on surface oxygen-containing functional groups and adsorption behavior of biochar, Chemosphere 207 (2018) 33–40.
[36] W. Chen, P. Westerhoff, J.A. Leenheer, K. Booksh, Fluorescence excitation-emission matrix regional integration to quantify spectra for dissolved organic matter, Environ. Sci. Technol. 37 (2015) 5701–5710.
[37] S. Yang, X. Yang, X. Shao, R. Niu, L. Wang, Activated carbon catalyzed persulfate oxidation of Azo dye acid orange 7 at ambient temperature, J. Hazard. Mater. 186 (2011) 659–666.
[38] X.-Y. Yu, Z.-C. Bao, J.R. Barker, Free radical reactions involving Cl•, Cl2-•, and SO4-• in the 248 nm photolysis of aqueous solutions containing S2O82- and Cl, J. Phys. Chem. A 108 (2004) 295–308.
[39] S. Wang, N. Zhou, Removal of carbamazepine from aqueous solution using sono-activated persulfate process, Ultrason. Sonochem. 29 (2016) 156–162.
[40] A. Georgi, F.-D. Kopinke, Interaction of adsorption and catalytic reactions in water decontamination processes: part I. Oxidation of organic contaminants with hydrogen peroxide catalyzed by activated carbon, Appl. Catal. B Environ. 58 (2005) 9–18.
[41] Y. Zhang, Q. Jiang, S. Jiang, H. Li, R. Zhang, J. Qu, S. Zhang, W. Han, One-step synthesis of biochar supported nZVI composites for highly efficient activating persulfate to oxidatively degrade atrazine, Chem. Eng. J. 420 (2021), 129868.
[42] D. Huang, Q. Zhang, C. Zhang, R. Wang, R. Deng, H. Luo, T. Li, J. Li, S. Chen, C. Liu, Mn doped magnetic biochar as persulfate activator for the degradation of tetracycline, Chem. Eng. J. 391 (2020), 123532.
[43] Q. Liu, X. Bai, X. Su, B. Huang, B. Wang, X. Zhang, X. Ruan, W. Cao, Y. Xu, G. Qian, The promotion effect of biochar on electrochemical degradation of nitrobenzene, J. Clean. Prod. 244 (2020), 118890.
[44] S. Liu, C. Lai, B. Li, C. Zhang, M. Zhang, D. Huang, L. Qin, H. Yi, X. Liu, F. Huang, X. Zhou, L. Chen, Role of radical and non-radical pathway in activating persulfate for degradation of p-nitrophenol by sulfur-doped ordered mesoporous carbon, Chem. Eng. J. 384 (2020), 123304.
[45] M. Cao, Y. Hou, E. Zhang, S. Tu, S. Xiong, Ascorbic acid induced activation of persulfate for pentachlorophenol degradation, Chemosphere 229 (2019) 200–205.
[46] J. Chen, X. Yu, C. Li, X. Tang, Y. Sun, Removal of tetracycline via the synergistic effect of biochar adsorption and enhanced activation of persulfate, Chem. Eng. J. 382 (2020).
[47] W. Huang, S. Xiao, H. Zhong, M. Yan, X. Yang, Activation of persulfates by carbonaceous materials: a review, Chem. Eng. J. 418 (2021).
[48] J. Song, S. Zhang, G. Li, Q. Du, F. Yang, Preparation of montmorillonite modified biochar with various temperatures and their mechanism for Zn ion removal, J. Hazard. Mater. 391 (2020), 121692.
[49] S. Zhang, Q. Du, Y. Sun, J. Song, F. Yang, D.C.W. Tsang, Fabrication of L-cysteine stabilized alpha-FeOOH nanocomposite on porous hydrophilic biochar as an effective adsorbent for Pb(2+) removal, Sci. Total Environ. 720 (2020), 137415.
[50] S. Li, F. Yang, Y. Zhang, Y. Lan, K. Cheng, Performance of lead ion removal by the three-dimensional carbon foam supported nanoscale zero-valent iron composite, J. Clean. Prod. 294 (2021).
[51] P. Shukla, B.S. Giri, R.K. Mishra, A. Pandey, P. Chaturvedi, Lignocellulosic biomass-based engineered biochar composites: a facile strategy for abatement of emerging pollutants and utilization in industrial applications, Renew. Sust. Energ. Rev. 152 (2021).
[52] D. Huang, H. Luo, C. Zhang, G. Zeng, C. Lai, M. Cheng, R. Wang, R. Deng, W. Xue, X. Gong, X. Guo, T. Li, Nonnegligible role of biomass types and its compositions on the formation of persistent free radicals in biochar: insight into the influences on Fenton-like process, Chem. Eng. J. 361 (2019) 353–363.
[53] S. Zhang, Q. Du, K. Cheng, M. Antonietti, F. Yang, Efficient phosphorus recycling and heavy metal removal from wastewater sludge by a novel hydrothermal humification-technique, Chem. Eng. J. 394 (2020).
[54] H. Lee, H.-i. Kim, S. Weon, W. Choi, Y.S. Hwang, J. Seo, C. Lee, J.-H. Kim, Activation of persulfates by graphitized nanodiamonds for removal of organic compounds, Environ. Sci. Technol. 50 (2016) 10134–10142.
[55] M. Kimura, I. Miyamoto, Discovery of the activated-carbon radical AC+ and the novel oxidation-reactions comprising the AC/AC+ cycle as a catalyst in an aqueous solution, Bull. Chem. Soc. Jpn. 67 (2006) 2357–2360.
[56] S. Wang, J. Wang, Activation of peroxymonosulfate by sludge-derived biochar for the degradation of triclosan in water and wastewater, Chem. Eng. J. 356 (2019) 350–358.
[57] D. Ouyang, Y. Chen, J. Yan, L. Qian, L. Han, M. Chen, Activation mechanism of peroxymonosulfate by biochar for catalytic degradation of 1,4-dioxane: important role of biochar defect structures, Chem. Eng. J. 370 (2019) 614–624.
[58] R. Yin, W. Guo, H. Wang, J. Du, Q. Wu, J.-S. Chang, N. Ren, Singlet oxygen-dominated peroxydisulfate activation by sludge-derived biochar for sulfamethoxazole degradation through a nonradical oxidation pathway: performance and mechanism, Chem. Eng. J. 357 (2019) 589–599.
[59] J. He, Y. Xiao, J. Tang, H. Chen, H. Sun, Persulfate activation with sawdust biochar in aqueous solution by enhanced electron donor-transfer effect, Sci. Total Environ. 690 (2019) 768–777.

Supporting Information

Removal of humic substances by the synergistic effect of biochar adsorption and activation of persulfate

Hongbo Liu[1*a], Mengting Ye[a], Xinyi Dong[a], Zhengxing Ren[a], Shiping Long[b], Eric Lichtfouse[c]

a School of Environment and Architecture, University of Shanghai for Science and Technology, 516 Jungong Road, 200093, Shanghai, China

b Chongqing New World Environment Detection Technology Co.LTD, 22 Jinyudadao, 401122, Chongqing, China

c Aix-Marseille Univ, CNRS, IRD, INRA, Coll France, CEREGE, 13100 Aix en Provence, France

1* Corresponding author ADD: 516, Jungong Road, 200093, Shanghai, China;

Email: Liuhb@usst.edu.cn (H., Liu) Tel: +86(21)55275979; Fax: +86(21)55275979

Table S1. Three-dimensional fluorescence area distribution.

Exitation (nm)	Emission (nm)	Representative compounds
200-250	280-380	Protein-like
200-250	380-550	Fulvic acids
250-450	280-380	Soluble microbial products
250-450	380-550	Humic acids

Table S2. Removal rate of HA after 120 min at different biochar dosage.

Biochar dosage (g/L)	0.1	0.3	0.5	0.7	0.9
Removal rate (%)	47.34	69.15	82.45	85.64	86.70

Table S3. Removal rate of HA after 180 min at different persulfate dosage.

Persulfate dosage (mM)	0.2	0.4	0.8	1	1.2	1.6	2
Removal rate (%)	70.15	79.31	84.49	85.06	83.91	84.48	80.46

Table S4. Removal rate of HA after 180 min at different initial pH.

Initial pH	5	6	7	8	9
Removal rate (%)	90.70	86.63	84.30	87.21	90.12

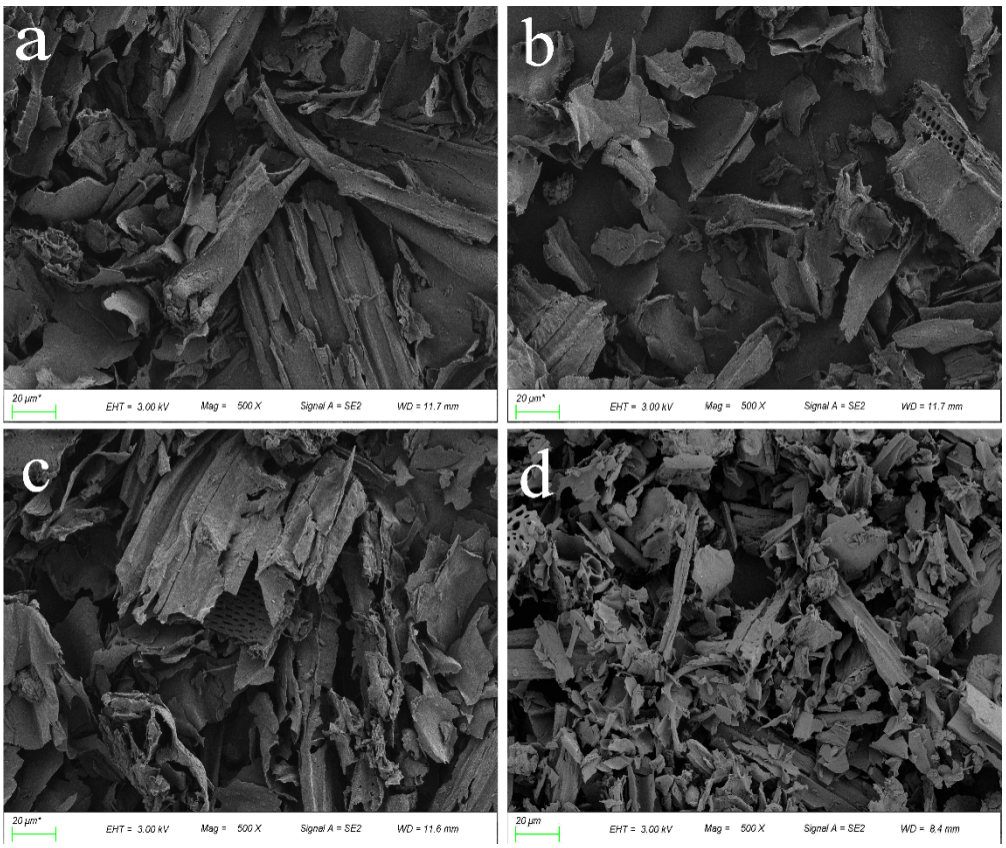

Fig. S1. SEM images of biochar produced at different pyrolysis temperature of (a) 400℃, (b) 600℃, (c) 700℃and (d) 900℃.

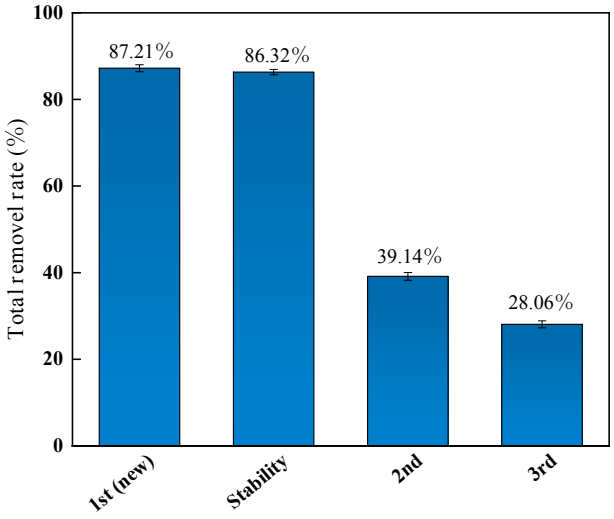

Fig. S2. Humic acids removal: effect of re-use (1st, 2nd, 3rd runs) and effect of stability after biochar storage during 6 months. Conditions: 5 mg/L humic acids, 0.5g/l biochar, 1 mM persulfate, pH 8.

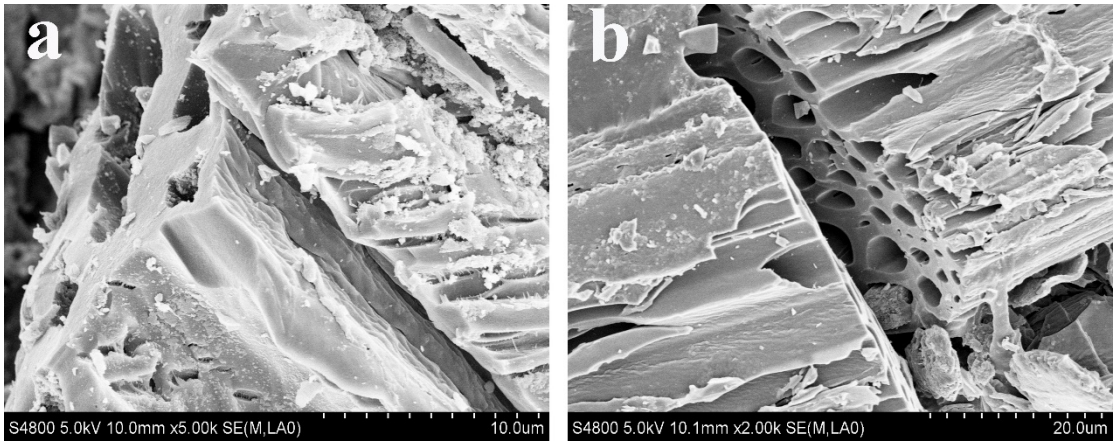

Fig. S3. Scanning electron microscopy (SEM) of the biochar surface after reaction of a) biochar and humic acids and b) biochar, persulfate and humic acids.

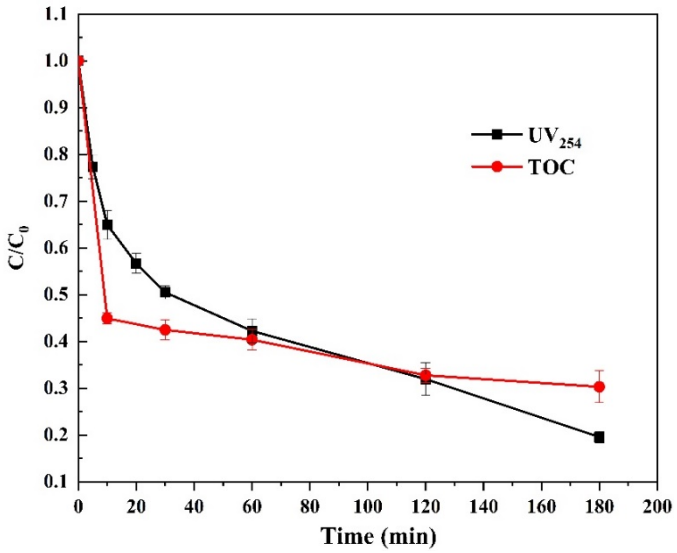

Fig. S4. Aqueous total organic carbon (TOC) removal of river water using 0.5 g/L biochar and 1 mM persulfate.